Rapid Radiotracer Washout from the Heart: Effect on Image Quality in SPECT Performed with a Single-Headed Gamma Camera System

Michael K. O'Connor and David S. Cho

Department of Radiology, Section of Nuclear Medicine, Mayo Clinic, Rochester, Minnesota

Technetium-99m-teboroxime demonstrates high extraction and rapid washout from the myocardium. To evaluate the feasibility of performing SPECT with this agent using a single-headed gamma camera system, a series of phantom studies were performed that simulated varying degrees of washout from normal and "ischemic" regions of the myocardium. In the absence of ischemic regions, short axis profiles were relatively unaffected by washout of <50% of activity over the duration of a SPECT acquisition. However, significant corruption of the SPECT data was observed when large (greater than a factor of 2) differences existed in the washout of activity from normal and "ischemic" myocardium. This corruption was observed with 30%–40% washout of activity from normal regions of the heart. Based on published washout rates, these results indicate that clinical studies with ^{99m}Tc-teboroxime may need to be completed within 2–4 min to order to prevent degradation of image quality due to differential washout effects.

J Nucl Med 1992; 33:1146–1151

Technetium-99m-teboroxime is a new myocardial perfusion agent, which demonstrates high myocardial extraction, rapid blood clearance and rapid washout from the myocardium (*1–3*). Animal studies have shown that the myocardial clearance rate ($T_{1/2}$ washout) of ^{99m}Tc-teboroxime varies from 7–12 min following exercise or dipyridamole to 10–20 min under resting conditions (*3–5*). This rapid washout presents a problem for conventional SPECT imaging of the heart as all reconstruction algorithms assume a static distribution of activity during the imaging period (*6,7*).

Although this problem can be resolved through the use of the new generation of multi-headed detector systems (*5,8*), these systems are not yet in widespread use. Several centers have performed SPECT imaging of ^{99m}Tc-teboroxime using single-headed gamma camera systems with a reduction in the total imaging time to approximately 10 min (*4,9*). This assumes that an imaging time comparable to the effective $T_{1/2}$ washout of ^{99m}Tc-teboroxime from the myocardium, will produce minimal distortion in the tomographic images (*4,9*). The validity of this assumption has not been determined, nor has any consideration been given to the effects of differential washout of ^{99m}Tc-teboroxime from normal and ischemic regions of the myocardium (*10,11*).

The purpose of this study was to determine in a phantom model: (a) the effects of washout per se and (b) the effects of differential washout on tomographic image quality using a single-headed gamma camera system.

MATERIALS AND METHODS

Study Design

In order to evaluate the effects of washout and differential washout on tomographic image quality, a model of the myocardium was selected that contained a large (50%) septal defect. The rationale for the selection of such a large defect, was to ensure that other factors that can influence image quality, such as imaging geometry, patient and table attenuation, scatter, phantom design and reconstruction parameters would be minimized relative to the extent and severity of the defect.

Cardiac Phantom

All studies were performed using a commercially available phantom (Model RH-2, Capintec, NJ). This phantom consisted of a lucite body (30 cm × 20 cm) with two compartments containing wood powder to simulate the lungs and a third central compartment in which a heart model could be positioned. The heart consisted of right and left ventricles with separate compartments for the blood pool and myocardium. Various plastic inserts could be placed into the myocardial compartment to simulate infarcted or ischemic myocardium.

Data Acquisition

A total of three acquisitions were performed. For each acquisition, the phantom was positioned in the center of the imaging table and orientated as for a conventional tomographic study of the heart. The exact position of the phantom on the table was marked to permit the phantom to be removed and re-positioned in the same orientation for each acquisition. For the three acqui-

Received Oct. 7, 1991; revision accepted Feb. 13, 1992.
For reprints contact: Dr. M. K. O'Connor, Section of Nuclear Medicine, Charlton Building, Mayo Clinic, Rochester, MN 55905.

sitions, ^{99m}Tc was placed in either the central compartment or the myocardium as outlined below.

Acquisition A. Three millicuries of ^{99m}Tc were placed as background activity in the central compartment—no heart phantom present.

Acquisition B. Three millicuries of ^{99m}Tc were placed in the myocardial compartment of heart phantom. No activity was placed in the central compartment, which was filled with water.

Acquisition C. Myocardial compartment of heart phantom contained a large defect (50% of total myocardial volume) centered over the septal region. Three millicuries of ^{99m}Tc were placed in the myocardial compartment. No activity was placed in the central compartment, which was filled with water.

All acquisitions were performed using a large field of view gamma camera (Orbiter 3700, Siemens Gammasonics, Des Plaines, IL) equipped with an low-energy general-purpose collimator. For each acquisition, a total of 32 images were acquired for 15 sec/image over 180°, beginning at 45° RAO and ending at 45° LPO. Data were stored in a 64 × 64 word mode matrix (Pinnacle System, Medasys Inc., Ann Arbor, MI).

Generation of Test Data

Acquisitions B and C were multiplied by a range of exponential decay functions to simulate washout of radioactivity from the myocardium. The data sets $B_0,B_{30},B_{50},B_{70},B_{90}$ and $C_0,C_{30},C_{50},C_{70},C_{90}$ were created, with the subscript indicating the percent washout of counts from the myocardium that occurred over the duration of the acquisition. From acquisition B, an additional group of data sets, $B_{15},B_{25},B_{35},B_{45}$, was created to study differential washout.

From an anterior view in study B, a region of interest was drawn around the myocardium and used to determine the average counts in the myocardial region for studies A, B and C. Approximate counts were 110,000 cts, 400,000 cts and 700,000 cts for studies A, B and C, respectively.

The planar data set A and the various data sets created above were combined in different proportions and with different washout rates to simulate a range of possible clinical studies. Table 1 describes the combinations used and the relative counts in the normal antero-lateral region and the "ischemic" septal region of the myocardium for each combination. A total of five washout levels were created in each study group. For all study groups, the myocardial-to-background ratio was approximately 4:1 at the start of each simulated acquisition. Figure 1 presents an example of the washout of activity from normal and "ischemic" myocardium for Group 3. The overall washout rate for a given study was determined by the relative contributions of counts from data sets A, B and C to total myocardial counts. Planar data set A contributed background activity to the heart. The addition of a

TABLE 1
Description of the Data Set Combinations Used To Generate the Five Study Groups and the Resulting Percent Activity in Both Normal and "Ischemic" Myocardial Zones at the Start and End of Each Study

Study group	Data set combinations	% Myocardial activity: Normal Start/End	% Myocardial activity: Ischemic Start/End	Description of study groups
	+ B_0	100/100	not applicable	Normal myocardium with washout during acquisition.
	+ B_{30}	100/75	not applicable	
1	A + B_{50}	100/51	not applicable	
	+ B_{70}	100/44	not applicable	
	+ B_{90}	100/28	not applicable	
	+ $C_0/4$	100/100	64/64	Moderate ischemic zone with no washout. Washout from normal myocardium.
	+ $C_{30}/4$	100/89	64/64	
2	A + $B_0/2$ + $C_{50}/4$	100/81	64/64	
	+ $C_{70}/4$	100/74	64/64	
	+ $C_{90}/4$	100/69	64/64	
	+ ($B_0/2$ + $C_0/4$)	100/100	64/64	As for Group 2, except ischemic washout rate = 0.5 normal washout rate.
	+ ($B_{15}/2$ + $C_{30}/4$)	100/82	64/58	
3	A + ($B_{25}/2$ + $C_{50}/4$)	100/71	64/54	
	+ ($B_{35}/2$ + $C_{70}/4$)	100/59	64/49	
	+ ($B_{45}/2$ + $C_{90}/4$)	100/48	64/45	
	+ ($B_0/2$ + $C_0/4$)	100/100	64/64	As for Group 2, except ischemic washout rate = 1.0 normal washout rate.
	+ ($B_{30}/2$ + $C_{30}/4$)	100/76	64/51	
4	A + ($B_{50}/2$ + $C_{50}/4$)	100/60	64/42	
	+ ($B_{70}/2$ + $C_{70}/4$)	100/44	64/34	
	+ ($B_{90}/2$ + $C_{90}/4$)	100/29	64/26	
	+ $C_0/2$	100/100	24/24	Severe ischemic zone with no washout. Washout from normal myocardium.
	+ $C_{30}/2$	100/76	24/24	
5	A + $C_{50}/2$	100/52	24/24	
	+ $C_{70}/2$	100/45	24/24	
	+ $C_{90}/2$	100/30	24/24	

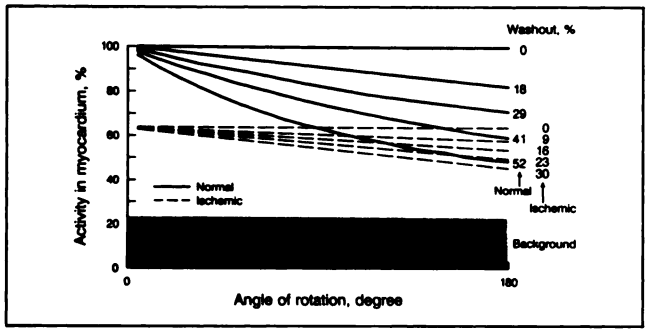

FIGURE 1. Example of the simulated washout of activity from normal and "ischemic" zones of the myocardium as a function of angle during a tomographic acquisition for Group 3.

monoexponential washout to this constant background gave a crude simulation of bi-exponential washout of myocardial activity. The percent activity in the myocardium at the start and end of each study is given in Table 1 for both normal and "ischemic" regions.

A total of 25 studies were produced from study Groups 1–5. All studies were reconstructed by prefiltering with a Hann filter (cut-off = 0.7 Nyquist) and backprojecting with a Ramp filter. From the transaxial data, conventional long and short axis slices of the heart were generated using the same orientation for all studies.

Data Analysis

Since the same reconstruction parameters were used for all studies, short-axis slices from identical regions of the myocardium could be compared between different studies. To reduce the volume of data to be processed, three representative short-axis slices were selected from the apex, mid-ventricle and base using selection criteria previously described (*12,13*). From these slices, circumferential count profiles were generated by noting the maximum pixel count along a ray line every 6° over 360°. To permit intercomparison of profiles, each profile was normalized to 100%, based on the maximum count in that profile. Errors introduced by washout of activity were quantitated by obtaining the ratio of profile counts in the "ischemic" zone to the normal zone. Average profile counts were calculated over 60° arcs centered at 90° and 270° for normal and "ischemic" myocardium, respectively.

RESULTS

Circumferential profiles of the mid-ventricular region from Groups 1–5 are presented in Figure 2. These indicate that significant changes in profile shape can occur as a result of washout for all studies. In most instances, the most significant changes occurred at washout levels in excess of 50% and are accompanied by distortion of the short-axis slices. At washout levels of 30%–40%, little or no distortion was observed in the image data. For a normal myocardium (Fig. 2A), washout of 50% or less of myocardial activity during the SPECT acquisition, leads to a drop of less than 10% in profile counts. For an abnormal myocardium, the presence of a differential washout rate between normal and "ischemic" regions appears to make the profile shape more sensitive to corruption (Fig. 2B, 2E).

The effects of differential washout on circumferential profile shape are more closely examined in Figure 3. Profiles are shown for apical, mid-ventricular and basal slices selected from Groups 2–4. The selected profiles were chosen to illustrate the effects of a 30%–40% washout of activity from normal regions of the myocardium over the duration of a SPECT acquisition. It can be seen that the most significant corruption of the circumferential profiles occurs when there is a large difference in washout rates between normal and "ischemic" myocardium. Table 2 presents the observed ratio of "ischemic"/normal activity

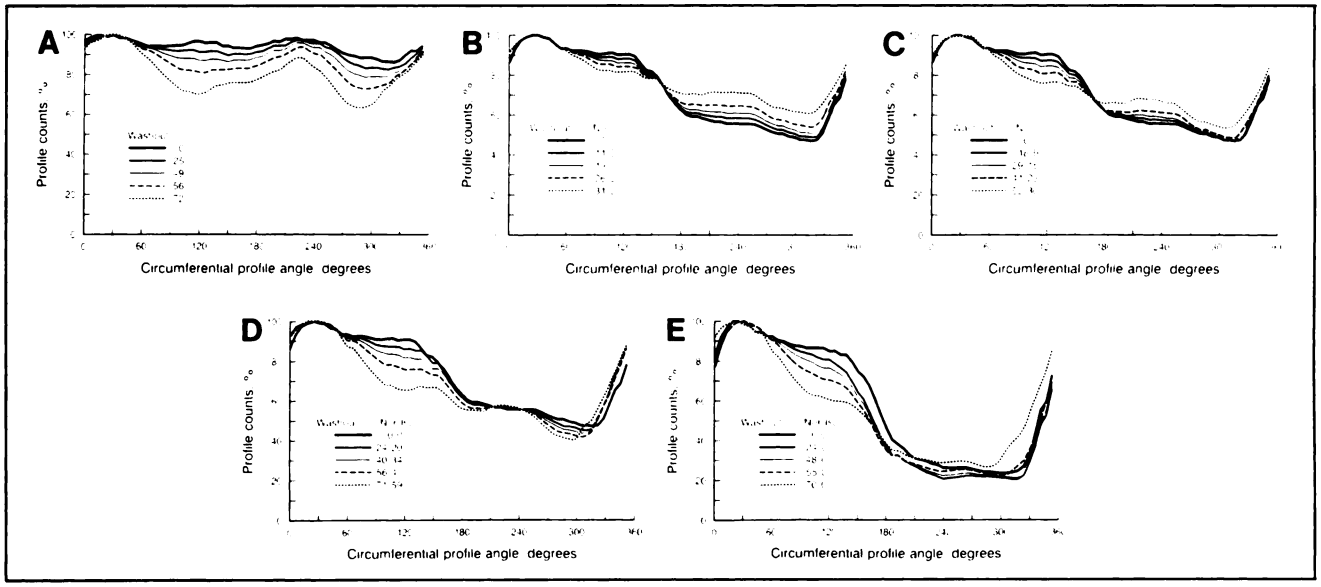

FIGURE 2. Circumferential profiles of the mid-ventricular short-axis slices for study Groups 1–5 described in Table 1 (2A–E, respectively). The percent washout of activity from normal (Nor) and "ischemic" (Isc) regions of the myocardium during each simulated acquisition is shown in the legends.

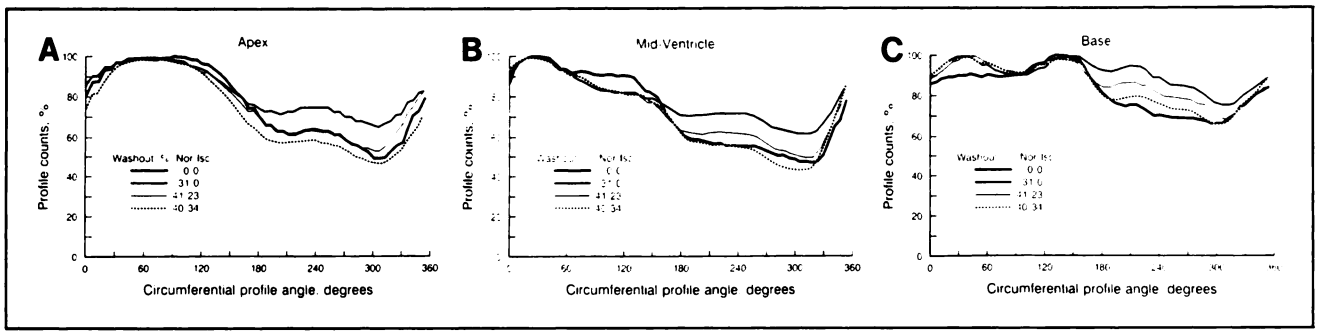

FIGURE 3. Effect of differential washout on circumferential profiles from (A) apical, (B) mid-ventricular and (C) basal short-axis slices. Slices were selected from study Groups 2–4 for cases in which the percent washout of activity from normal (Nor) and "ischemic" (Isc) regions of the myocardium during each simulated acquisition was less than approximately 40%.

for the three selected slices at different washout levels. For the worst case studied, i.e., 30% washout from normal myocardium and 0% washout from "ischemic" myocardium, there were errors of between 26%–39% in the observed ratio.

Figure 4 presents the short-axis slices corresponding to the circumferential profiles shown in Figure 3. Within the "ischemic" region of the myocardium, there is a gradual fill-in of activity as the difference in washout rates between normal and "ischemic" regions increases. In the extreme case where there is no washout from the "ischemic" region (Fig. 4, second row), the apparent increase in activity in this region is sufficient to alter the interpretation of these images.

DISCUSSION

Variations in organ activity over the duration of a tomographic acquisition are not generally of major concern, due to the stable distribution of most radiopharmaceuticals used in SPECT. One of the most troublesome causes of changing activity has been bladder filling during bone SPECT of the pelvis. While this problem has been addressed in a number of studies, these have been concerned with the elimination of this activity, rather than examining the distortion of bladder activity itself (*14,15*).

A study by Bok et al. (*16*) has examined the effects of varying activity in a line source on the quality of the tomographic reconstruction of that source. They found that distortion was only visible if washout levels exceeded 50% over a 360° orbit. The degree of distortion also increased if the orbit was reduced from 360° to 180°. Clinical studies on ^{99m}Tc-teboroxime myocardial imaging have referenced this study as a guide to the degree of washout that can be tolerated before corruption of image data occurs (*4,9*). In the absence of differential washout, our results are in agreement with the findings of Bok et al. (*16*), in that visual inspection of the short-axis slices did not show any significant image distortion, provided that washout levels did not exceed 50% for any part of the myocardium. These findings have also been confirmed in a phantom study by Li et al. (*17*).

Unfortunately, these simple washout models may not give a good representation of the kinetics of ^{99m}Tc-teboroxime in normal and diseased myocardium. Studies by Stewart et al. in a dog model have shown that the pattern of washout of ^{99m}Tc-teboroxime from the myocardium is a complex one that is bi-exponential and highly dependent on blood flow (*5,18*). These studies showed that after pharmacologic stress, the first washout $T_{1/2}$ component varied from 5–6 min in normal regions to 10–12 min in occluded regions (*18*). The washout $T_{1/2}$ of the second component has not been well defined and in dogs seems to range between 0.5–2.5 hr (*10*). A biexponential washout of myocardial activity has also been reported in studies on normal volunteers (*4*). Washout $T_{1/2}$ components of 5.2 min and 3.8 hr were observed, representing approximately 66% and 33% of myocardial activity, respectively.

Recently, a computer simulation study has been performed by Links et al. (*19*) that examines the question of differential washout from normal and "ischemic" regions of the heart. They studied small apical and lateral wall defects using washout $T_{1/2}$ values determined from dog studies. Their study indicated that SPECT acquisitions of longer than 3 min resulted in image artifacts and errors in quantitation. In contrast to that study, we examined the effects of a variety of differential washout rates on a single large septal defect. Our results support their findings and indicate that differential washout is the critical factor in determining the degree of corruption to the image data (Fig. 3B–E). Figure 4 shows that as differential washout increases, there is a loss in contrast between normal and "ischemic" regions which significantly reduces the ability to detect an "ischemic" lesion. Furthermore, there are subtle changes in the appearance of the normal regions which can be appreciated from the mid-ventricular and basal images in Figure 4. Similar changes in the apparent activity in normal myocardium were noted in the study of Links et al. (*19*).

Initial clinical studies with ^{99m}Tc-teboroxime have found varying sensitivity and specificity when compared to ^{201}Tl. While some studies have shown superior results (*20,21*), in general, results with ^{99m}Tc-teboroxime have been similar

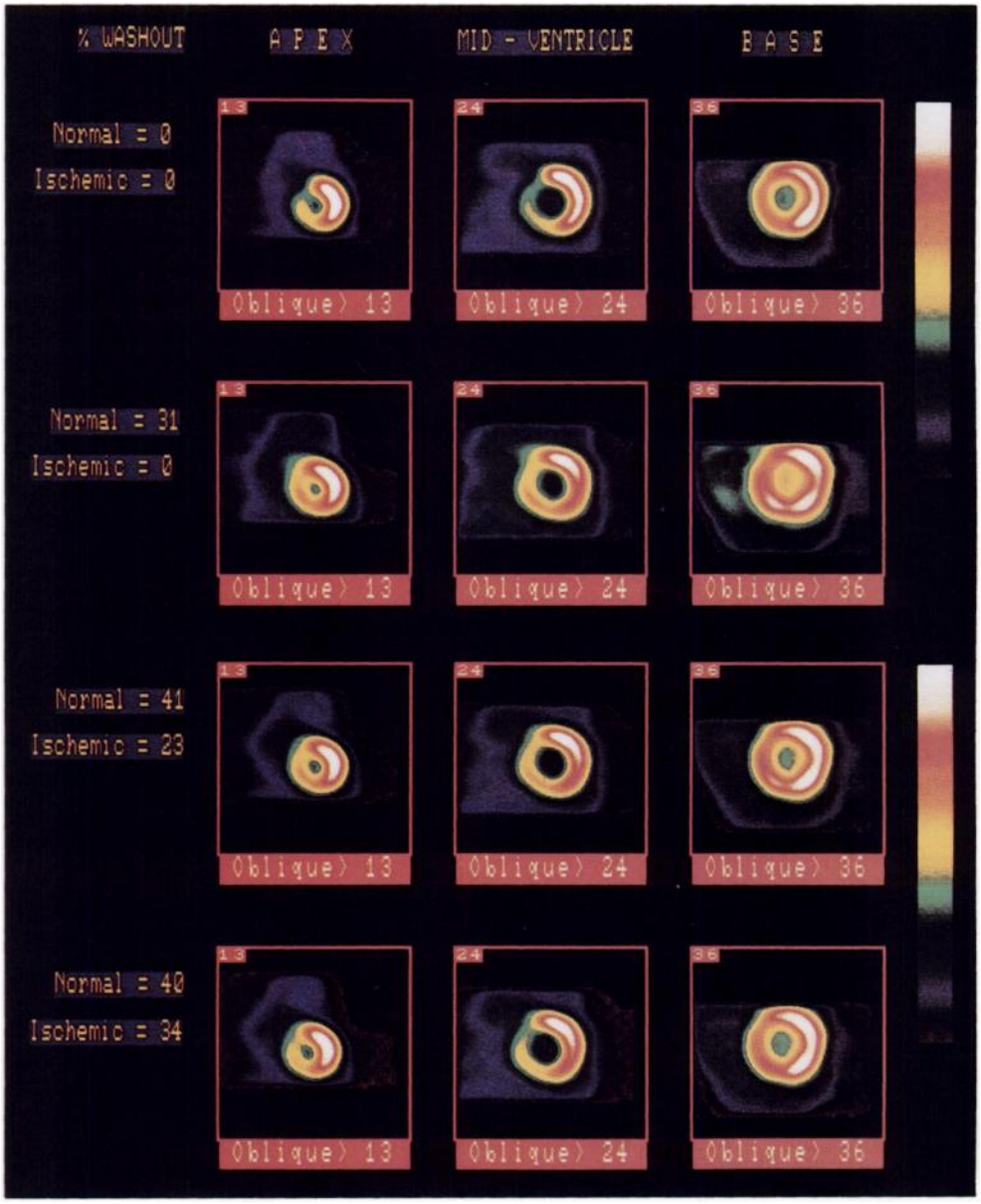

FIGURE 4. (A) Apical, (B) mid-ventricular and (C) basal short-axis slices corresponding to the circumferential profiles in Figure 3. All images are scaled to their own minimum and maximum.

or slightly poorer than ^{201}Tl, despite the superior imaging characteristics of ^{99m}Tc (*22–26*). Much of the variability in clinical results seen with teboroxime may be due to differences in the methods and duration of image acquisition. A recent study by Bontemps et al. (*23*) has found that in cases of discordant findings between ^{99m}Tc-teboroxime and ^{201}Tl myocardial scans, the majority showed normal ^{99m}Tc-teboroxime uptake with corresponding abnormal ^{201}Tl uptake. This loss of sensitivity for the detection of reversible ischemia may be due to differential washout effects. The importance of washout has been noted by Iles et al. (*24*). Their study showed that shortening the acquisition time from 6 min to 3–4 min resulted in better agreement between ^{201}Tl and ^{99m}Tc-teboroxime studies.

Assuming, in clinical studies, that Tc-99m teboroxime has a bi-exponential washout with $T_{1/2}$'s of approximately 5 min and 2–3 hr for normal myocardium following stress, then 30%–40% washout of activity would occur with a SPECT acquisition of <5 min duration. Hence, the data presented in Table 2 and Figures 3 and 4 can be used as indicators of the possible effects of differential washout on ^{99m}Tc-teboroxime image quality during a 5-min SPECT acquisition. These results indicate that significant changes occur in the distribution of counts within short-axis images for a large septal defect. The study of Links et al. (*19*) found similar changes for small apical and lateral wall lesions. Neither of these phantom studies fully explore the range of lesions sizes, locations and the variations in acquisition times and differential washout rates that may occur in clinical studies. Clearly, further work is needed to clarify the relative differences in washout rates between normal and "ischemic" regions of the myocardium in clinical studies, and how these washout rates vary with the

TABLE 2
Ratio of Myocardial Activity in "Ischemic" (Isc) and Normal (Nor) Regions for the Short-Axis Slices Presented in Figure 4

Short-Axis slice	%Washout Isc/Nor	Observed Isc/Nor ratio*	%Error
Apex	0/0 (no washout)	0.57	—
Apex	40/34	0.55	−3.5%
Apex	41/23	0.60	5.3%
Apex	31/0	0.72	26.3%
Mid-ventricular	0/0 (no washout)	0.57	—
Mid-ventricular	40/34	0.57	0.0%
Mid-ventricular	41/23	0.65	14.0%
Mid-ventricular	31/0	0.79	38.6%
Base	0/0 (no washout)	0.73	—
Base	40/34	0.76	4.1%
Base	41/23	0.83	13.7%
Base	31/0	0.90	23.3%

* True ratio of "ischemic"/normal activity = 0.64.

For each slice, errors are expressed as percent difference in activity for different washout levels relative to no washout.

type of stress (i.e., exercise or pharmacologic). This can best be done with the multi-headed detector systems, because their short acquisition times (<2 min) will permit the determination of washout rates for normal and "ischemic" regions of the myocardium.

Based on phantom studies and initial clinical results with teboroxime, it would appear that ^{99m}Tc-teboroxime studies are highly susceptible to corruption of the image data. The degree to which the image data may be corrupted will depend on the differential washout rate for normal and ischemic myocardium and on the duration of acquisition. Acquisition times as short as 2–4 min may be required in order to reduce image corruption below levels that are clinically significant. As the kinetics of teboroxime in normal and ischemic myocardium become better defined, it will be possible to more accurately determine the limits under which single-headed systems can be used to image this agent.

REFERENCES

1. Seldin DW, Johnson LL, Blood DK, et al. Myocardial perfusion imaging with technetium-99m SQ30217: comparison with thallium-201 and coronary anatomy. *J Nucl Med* 1989;30:312–319.
2. Coleman RE, Maturi M, Nunn AD, Eckelman WC, Juri PN, Cobb FR. Imaging of myocardial perfusion with SQ30217: dog and human studies [Abstract]. *J Nucl Med* 1986;27:893.
3. Narra RK, Nunn AD, Kuczynski BL, Feld T, Wedeking P, Eckelman WC. A neutral technetium-99m complex for myocardial imaging. *J Nucl Med* 1989;30:1830–1837.
4. Johnson LL, Seldin DW. Clinical experience with technetium-99m teboroxime, a neutral, lipophilic myocardial perfusion imaging agent. *Am J Cardiol* 1990;66:63E–67E.
5. Stewart RE, Schwaiger M, Hutchins GD, et al. Myocardial clearance kinetics of technetium-99m-SQ30217: a marker of regional myocardial blood flow. *J Nucl Med* 1990;31:1183–1190.
6. Brooks RA, Di Chiro G. Principles of computer assisted tomography (CAT) in radiographic and radioisotope imaging. *Phys Med Biol* 1976;21: 689–732.
7. Budinger TF, Gullberg GT, Huessman RH. Emission computed tomography. In: Herman GT, ed. *Image reconstruction from projections.* Berlin: Springer-Verlag; 1979:147–246.
8. Nakajima K, Taki J, Bunko H, et al. Dynamic acquisition with a three-headed SPECT system: application to technetium-99m-SQ30217 myocardial imaging. *J Nucl Med* 1991;32:1273–1277.
9. Johnson LL. Clinical experience with technetium-99-teboroxime. *Semin Nucl Med* 1991;21:182–189.
10. Glover DK, Okada RD, Hebert CB. Tc-99m-teboroxime (SQ30217, Cardiotec) kinetics in normal and ischemic canine myocardium [Abstract]. *Circulation* 1990;82:III–486.
11. Miller DD, Stewart RE, Heyl B, O'Rourke RA. Diagnostic accuracy of differential post-stenotic myocardial technetium-99m teboroxime clearance following non-exercise cardiac stress [Abstract]. *J Nucl Med* 1991; 32:947–948.
12. O'Connor MK, Hammell T, Gibbons RJ. In vitro validation of a simple tomographic technique for estimation of percentage myocardium at risk using methoxyisobutyl isonitrile technetium-99m (sestamibi). *Eur J Nucl Med* 1990;17:69–76.
13. Gibbons RJ, Verani MS, Behrenbeck T, et al. Feasibility of tomographic ^{99m}Tc-hexakis-2-methoxy-2-methylpropyl-isonitrile imaging for the assessment of myocardial area at risk and the acute effect of treatment in acute myocardial infarction. *Circulation* 1989;80:1277–1286.
14. O'Connor MK, Kelly BJ. Evaluation of techniques for the elimination of "hot" bladder artifacts in SPECT of the pelvis. *J Nucl Med* 1990;31: 1872–1875.
15. Gillen GJ, McKillop JH, Hilditch TE, Davidson JK, Elliott AT. Digital filtering of the bladder in SPECT bone studies of the pelvis. *J Nucl Med* 1988;29:1587–1595.
16. Bok BD, Bice AN, Clausen M, Wong DF, Wagner HN. Artifacts in camera-based single photon emission tomography due to time activity variation. *Eur J Nucl Med* 1987;13:439–442.
17. Li QS, Solot G, Frank TL, Wagner HN, Becker LC. Tomographic myocardial perfusion imaging with technetium-99m-teboroxime at rest and after dipyridamole. *J Nucl Med* 1991;32:1968–1976.
18. Stewart RE, Heyl B, O'Rourke RA, Blumhardt R, Miller DD. Demonstration of differential post-stenotic myocardial technetium-99m-teboroxime clearance kinetics after experimental ischemia and hyperemic stress. *J Nucl Med* 1991;32:2000–2008.
19. Links JM, Frank TL, Becker LC. Effect of differential tracer washout during SPECT acquisition. *J Nucl Med* 1991;32:2253–2257.
20. Fleming RM, Kirkeeide RL, Taegtmeyer H, Adyanthaya A, Goldstein RA. Tc-99m teboroxime SPECT imaging: comparison to thallium-201 and quantitative coronary arteriography [Abstract]. *Circulation* 1990;82: III–652.
21. Hendel RC, McSherry BA, Leppo JA. The detection and differentiation of myocardial ischemia and infarction by teboroxime compared with thallium (with and without reinjection) [Abstract]. *Eur J Nucl Med* 1991;18:539.
22. Kim AS, Akers MS, Faber TL, Corbett JR. Dynamic myocardial perfusion imaging with Tc-99m teboroxime in patients: comparisons with thallium-201 and arteriography [Abstract]. *Circulation* 1990;82:III–321.
23. Bontemps L, Geronicola-Trapali X, Sayegh Y, Delmas O, Itti R, Andre-Fouet X. Myocardial scintigraphy with technetium-99m teboroxime: comparison with thallium-201 [Abstract]. *Eur J Nucl Med* 1991;18:539.
24. Iles S, Lalonde L, Fung A, et al. Exercise Tc-99m teboroxime cardiac SPECT: optimization of acquisition parameters [Abstract]. *Eur J Nucl Med* 1991;18:648.
25. Burns RJ, Fung A, Iles S, et al. Exercise Tc-99m teboroxime cardiac SPECT: results of a Canadian multicenter trial [Abstract]. *Eur J Nucl Med* 1991;18:539.
26. Taillefer R, Freeman M, Greenberg D, et al. Comparison between ^{99m}Tc-teboroxime and ^{201}Tl planar myocardial imaging in the detection of coronary artery disease in a Canadian multicenter trial [Abstract]. *Eur J Nucl Med* 1991;18:656.